Published in final edited form as:
Ultrasound Med Biol. 2015 January ; 41(1): 187–196. doi:10.1016/j.ultrasmedbio.2014.08.018.

Shaken and stirred: mechanisms of ultrasound-enhanced thrombolysis

Kenneth B. Bader[1], **Matthew J. Gruber**[2], and **Christy K. Holland**[1,2]

[1]Department of Internal Medicine, Division of Cardiovascular Disease and Health, University of Cincinnati, University of Cincinnati, Cincinnati, OH, USA

[2]Biomedical Engineering Program, University of Cincinnati, Cincinnati, OH, USA

Abstract

The use of ultrasound and microbubbles as an effective adjuvant to thrombolytics has been demonstrated *in vitro*, *ex vivo*, and *in vivo*. However, the specific mechanisms of ultrasound-enhanced thrombolysis (UET) have yet to be elucidated. We present visual observations illustrating two mechanisms of UET: acoustic cavitation and radiation force. An *in vitro* flow model was developed to observe human whole blood clots exposed to human fresh-frozen plasma, rt-PA (0, 0.32, 1.58, or 3.15 μg/mL), and the ultrasound contrast agent Definity® (2 μL/mL). Intermittent, continuous-wave, ultrasound (120 kHz, 0.44 MPa peak-to-peak pressure) was used to insonify the perfusate. Ultraharmonic (UH) emissions indicative of stable cavitation were monitored with a passive cavitation detector. The clot was observed with an inverted microscope, and images were recorded with a charge-coupled device (CCD) camera. The images were post processed to determine the time-dependent clot diameter and root-mean-square velocity of the clot position. Clot lysis occurred preferentially surrounding large, resonant-sized bubbles undergoing stable oscillations. UH emissions from stable cavitation were found to correlate with the lytic rate. Clots were observed to translate synchronously with the initiation and cessation of the ultrasound exposure. The root-mean-square velocity of the clot correlated with the lytic rate. These data provide visual documentation of stable cavitation activity and radiation force during sub-megahertz sonothrombolysis. The observations of this study suggest that the process of clot lysis is complex, and both stable cavitation and radiation force are mechanistically responsible for this beneficial bioeffect in this *in vitro* model.

Keywords

Acute ischemic stroke; Ultrasound; Ultrasound Contrast Agents; Acoustic Cavitation

Introduction

Stroke is currently the fourth leading cause of death in the United States of America (Go et al., 2013). At present, the only thrombolytic therapy that is approved by the FDA for the treatment of ischemic stroke is recombinant tissue-type plasminogen activator (rt-PA).

Corresponding Author contact: Kenneth B. Bader, 231 Albert Sabin Way, CVC 3933, Cincinnati, OH 45267-0586, kenneth.bader@uc.edu, Phone: 513-558-8990.

However, this potent thrombolytic is only administered in 1.5% of cases (Go et al., 2013) due to potential bleeding complications and strict contraindication criteria (Turi et al., 1993). Adjuvant therapies that lower the dose of rt-PA or increase efficacy would represent an important breakthrough. Ultrasound-enhanced thrombolysis (UET) has shown potential for both.

The efficacy of UET has been demonstrated in vitro (Cheng et al., 2005; Datta et al., 2008; Prokop et al., 2007) and in clinical trials (Alexandrov et al., 2004; Molina et al., 2009), but the specific mechanisms of UET have yet to be elucidated. Enhancement of thrombolysis is thought to be primarily mechanical in nature (Blinc et al., 1993; Francis et al., 1992; Shaw et al., 2007). Acoustic streaming, generated by absorption of the ultrasonic energy (Nyborg, 1953), increases penetration of rt-PA into the clot (Francis et al., 1995) or radiation force displaces of the clot (Devcic-Kuhar et al., 2002). Acoustic cavitation, or the nucleation and generation of bubble activity caused by an acoustic source (Apfel, 1981), has been shown to enhance thrombolytic efficacy (Everbach and Francis, 2000). Acoustic emissions from stable cavitation, characterized by gentle nonlinear oscillations of the bubble (Flynn, 1964), have previously been correlated to the enhancement of rt-PA thrombolysis (Datta et al., 2008; Prokop et al., 2007). These stable bubbles are known to induce small-scale streaming, termed microstreaming (Elder, 1959), which is thought to facilitate increased penetration of rt-PA into the thrombous (Datta et al., 2008). Additionally, microstreaming is thought to remove fibrin-degradation products, which increases the availability of plasminogen binding sites for rt-PA (Sutton et al., 2013).

However, previous studies did not provide real-time measurement of the lytic rate, which would enable the identification of the mechanisms of thrombolytic enhancement. To overcome this difficulty, Cheng et al. (2005) developed an *in vitro* model to observe thrombolysis in real time. This model was extended by Gruber et al. (2014) to include fluid flow past the clot, a potentially important aspect of the lytic rate (Bajd and Serša, 2012), to allow replenishment of cavitation nuclei (Hitchcock et al., 2011). The ability to detection bubble activity optically and track the movement of the clot has recently been integrated into this measurement system, in order to probe the relationship between lytic rate, cavitation, and clot movement.

Materials and Methods

Preparation of human fresh frozen plasma and recombinant tissue-type plasminogen activator

Human fresh-frozen plasma (hFFP) was procured from a blood bank (Hoxworth Blood Center, Cincinnati, OH). Thirty milliliter aliquots of the hFFP were thawed for each experiment and allowed to reach atmospheric gas equilibrium at 37 °C in an open container for two hours. Recombinant tissue-type plasminogen activator (rt-PA) was obtained from the manufacturer (Activase®, Genentech, San Fransisco, CA, USA) as lyophilized power. Each vial was mixed with sterile water to a concentration of 1 mg/mL as per manufacturer instructions, aliquoted into 1.0 mL centrifuge tubes, and stored at −80 °C. The enzymatic activity of rt-PA is stable over a period of 7 years using this protocol (Shaw et al., 2009b).

Preparation of blood clots

Human whole blood clots were manufactured around silk sutures following a protocol developed by Shaw et al. (2008). Following local Institutional Review Board approval and written informed consent, venous human whole blood was drawn from a pool of 5 healthy volunteers. Aliquots of 500 μL were transferred to sterile glass tubes containing borosilicate glass micropipettes (1.12 mm inner diameter, World Precision Instruments, Inc., USA), pre-threaded with 7–0 silk sutures (Ethicon Industries, Cornelia, GA). The blood was allowed to clot around the silk suture at 37 °C for 3 hours. Following clot formation, the tubes were stored at 5 °C for a minimum of 3 days to allow for maximal clot retraction (Shaw et al., 2009a), lytic resistance, and stability (Shaw et al., 2006). Before each measurement, the micropipette was removed to produce a cylindrical clot adherent to the suture. The initial clot size (550 μm ± 43 μm) was smaller than that of the middle cerebral artery (MCA) (2.4 mm − 4.6 mm (Ng et al., 2007; Saqqur et al., 2007)), the site of occlusion for the majority of ischemic strokes (Gibo et al., 1981). However, the clot size is comparable to intracerebral perforating branches of the MCA (80–840 μm (Marinkovic et al., 1985)), which are highly vulnerable to occlusion.

Preparations of ultrasound contrast agents (UCAs)

Vials of Definity® (perflutren lipid microspheres; Lantheus Medical Imaging, N. Billerica, MA, UCA), microbubbles consisting of octofluoropropane encapsulated by a lipid shell monolayer, were activated according to the manufacturer's instructions. The vial was stored at 5 °C until needed. The vial was allowed to warm to room temperature (20−24°C) for one hour prior to activation by shaking for 45 seconds using a Vial-Mix® (Lantheus Medical Imaging). The agent was diluted to a final concentration of 2 μL/mL (1×10^4 particles/mL). This number density is consistent with the manufacturer's recommended dose (Lantheus Medical Imaging, Billerica, MA, USA) for left ventricular opacification.

In vitro flow phantom

The *in vitro* flow model based on Cheng et al. (2005) and Gruber et al. (2014) used to quantify thrombolytic efficacy and bubble activity is depicted in Fig. 1. An acrylic tank (16 cm × 33 cm × 9 cm) was filled with approximately 3 L of degassed (20 ± 5% dissolved oxygen), reverse-osmosis water heated to 37.3 ± 0.3 °C. The water was filtered (0.2 μm), and the gas content and temperature were maintained throughout the experiment with a custom-built recirculation system. The walls of the tank were lined with a 1 cm thick acoustic absorber (Aptflex F48, Precision Acoustics, Dorchester, Dorset, UK).

The flow channel consisted of low-density polyethylene tubing (inner diameter 1.6 mm, outer diameter 3.2 mm, part 1J-109-10, Freelin Wade Co., McMinnville, OR, USA) to direct the perfusate from a reservoir to a glass micropipette (2.15 mm inner diameter, 0.3 mm wall thickness 5-000-2200, Drummond Scientific Co., Broomall, PA, USA). A clot was mounted along the central axis of the micropipette by snuggly fitting the suture at the ends of the micropipette with latex tubing. The micropipette was positioned over a microscope slide (Fisherbrand, 12-550C, Fisher Scientific, Pittsburg, PA, USA) in the bottom of the tank to allow imaging of the clot with an inverted microscope (IX71, Olympus Corporation, Center Valley, PA, USA). The focal area of the objective (UPlanFLN 10×, 10 mm working

distance, Olympus Corporation, Center Valley, PA, USA) was approximately 1200 μm × 900 μm. Images were captured by a CCD camera (Retiga-2000R, Q Imaging, Surrey, BC, Canada) at a rate of 2.33 Hz. Flow was maintained at 0.65 mL/min with a programmable syringe pump (model 44, Harvard Apparatus Co. Inc., South Natick, MA) in continuous withdrawal mode. This flow rate is in the range of physiologic flow rates measured in the occluded middle cerebral artery during ischemic stroke (Alexandrov et al., 2010).

Clot diameter and position

Images of the clots were used to determine the lytic rate (Cheng et al., 2005). The Sobel approximation (Gonzalez and Woods, 2002) was used to determine the spatial gradient of each gray scale image. The clot edges were determined by determined by an edge-detection routine following Meunier et al. (2007). The clot diameter for a given frame, $\overline{d}$, was defined as average distance between detected edges for each pixel row of the image (600 rows total, 900 μm total length), minus the diameter of the suture (95 μm ± 15 μm) (Shaw et al., 2009a).

The lytic rate was defined as the ratio of the change of the clot diameter, $\Delta\overline{d}$, to the change in time, Δ*t*:

$$\frac{\Delta\overline{d}}{\Delta t}=\frac{1}{t_2-t_1}\frac{\overline{d}(t_2)-\overline{d}(t_1)}{\overline{d}(t_0)} \quad (1)$$

where $\overline{d}(t)$ is the clot diameter at time *t*, the subscripts indicate initial (1) and final (2) time points over which the lytic rate was calculated, and $\overline{d}\,(t_0)$ indicates the clot diameter at time *t* = 0. The position of the clot for a given frame was defined as the average location of the center of the clot determined over the entire length of the clot in the image. Movement of the clot was quantified by the root-mean-square (RMS) velocity of the clot position, v_{RMS}:

$$v_{RMS}=\sqrt{\frac{1}{t_2-t_1}\int_{t_1}^{t_2}dt\left(\frac{x\,(t_2)-x\,(t_1)}{t_2-t_1}\right)^2} \quad (2)$$

where *x*(*t*) denotes the position of the clot at time, *t*, and the subscripts indicate initial (1) and final (2) time points over which the RMS velocity is being calculated.

Ultrasound exposure and cavitation detection

A custom-designed transducer (H160, Sonic Concepts, Inc. Woodburn, WA, USA) was used to insonate the clot and perfusate. The unfocused transducer element (30 mm diameter aperture) was excited at its resonant frequency of 120 kHz with a function generator (33250A, Agilent Technologies, Inc., Santa Clara, CA, USA) and power amplifier (1040L, ENI, Rochester, NY, USA). A custom-built impedance matching network (Sonic Concepts, Inc. Woodburn, WA, USA) maximized power transfer to the transducer. The acoustic field was measured along the clot with a 0.5-mm hydrophone (TC 4038, Teledyne Reson Inc. Goleta, CA, USA) mounted on a computer-controlled three-axis positioner (NF-90, Velmex Inc., Bloomfield, NY, USA).

Ultraharmonic (UH) emissions, a key acoustic signature of stable cavitation (Datta et al., 2008; Hitchcock et al., 2011), and broadband (BB) emissions, characteristic of inertial cavitation (Datta et al., 2008), were monitored with a passive cavitation detector (PCD) aligned confocal with the clot. The PCD, a 19-mm-diameter circular single-element, long-focus 2.25-MHz transducer (595516C, Picker Roentgen GmbH, Espelkamp, Germany), has previously been utilized to detect cavitation at 120 kHz (Datta et al., 2008; Hitchcock et al., 2011). The received signal from the PCD was filtered by a 10-MHz low-pass filter (J73E, TTE Inc, Los Angeles, CA, USA) to halt noise from radiofrequency interference, and amplified with a wideband low-noise amplifier (CLC100, Cadeka Microcircuits LLC, Colorado, USA). The signal was digitized (10 ms duration, 31.25 MHz sampling frequency), and the power spectrum computed in MATLAB® (The Mathworks, Natick, MA, USA). Ultraharmonic bands (Hitchcock et al., 2011) of the power spectrum between 250 kHz and 1 MHz were summed over a 2-kHz bandwidth centered around the UH. Broadband emissions in the received signal were summed in 4 kHz bands centered at each UH ± 10 kHz and ± 30 kHz. These UH and BB bands were found to have a signal-to-noise ratio greater than 3 decibels (Gruber et al., 2014).

An intermittent ultrasound exposure scheme was utilized following Hitchcock et al. (2011). A peak-to-peak pressure of 0.44 MPa and insonation period of 50 s were found to maximize UH emissions and minimize broadband emissions, indicative of inertial cavitation (Datta et al., 2006), over the 30 min treatment duration. The insonation period was followed by a 30 s quiescent period to allow a fresh influx of Definity® to fill the micropipette. The optimized insonation period and quiescent period were repeated in succession until the duration of the 30 min treatment.

Experimental Procedure

A clot was mounted in the capillary tube, and submerged in the temperature-controlled fluid within the tank. The position of the tank was adjusted so that the clot was positioned over the microscope objective. The focus of the PCD was aligned with the capillary tube. Clots were treated for 30 minutes with hFFP infused with rt-PA alone, rt-PA and the optimized intermittent ultrasound scheme (0.44 MPa peak-to-peak continuous wave, 50 s on, 30 s off), or rt-PA and the optimized intermittent ultrasound scheme and Definity® (2 μL/mL). Each treatment investigated rt-PA concentrations of 0 μg/mL, 0.32 μg/mL, 1.58 μg/mL, and 3.15 μg/mL. Images and acoustic emissions recorded by the PCD were acquired at a rate of 2.3 Hz (0.43 s inter-frame time), and stored for analysis offline.

Correlation statistics

The reduction in clot diameter was correlated with UH emissions and the RMS velocity of the clot using the Spearman's rank correlation coefficient in MATLAB® (The Mathworks, Natick, MA, USA). A four-second moving average was applied to the time series data (e.g. change in clot diameter, UH emissions, or RMS velocity) prior to calculating the correlation. The four-second window of the moving average was the minimum window duration required to remove error in the image analysis associated with flowing lysed clot particulates. The hypothesis of no correlation against the alternative that there is a nonzero correlation was disproved for *p*-values less than 0.05.

Results

For all concentrations of rt-PA, the lytic rate over the 30 min treatment was greatest when rt-PA and Definity® were exposed to submegahertz-frequency ultrasound, as shown in Fig. 2, due to sustained cavitation. A rich variety of bubble activity was observed during the insonation of Definity® (Videos 1–3). Resonant-sized bubbles (53 μm ± 19 μm, n = 50) were formed via coalescence during acoustic excitation, as shown in Fig. 3. The pixel intensity increased rapidly around the bubble during insonation, indicating local lysis of the clot (Cheng et al., 2005), as shown in Fig. 4. The increase in pixel intensity surrounding the bubble occurs over several seconds (Fig. 4a–4c), which constitutes over one million acoustic periods.

Sustained bubble activity is characteristic of stable cavitation. Stable oscillations of the bubble were further evidenced by the presence of UH acoustic emissions during clot lysis (Videos 1–3). The energy of the UH emissions was found to correlate significantly ($p < 0.05$) with the instantaneous lytic rate (Fig. 5a). Such cavitation activity was only beneficial in the presence of rt-PA, however. No correlation between the instantaneous lytic rate and UH emissions was observed in the absence of rt-PA (Fig. 5a and Video 4). The instantaneously lytic rate correlated significantly ($p < 0.05$) with broadband emissions at all concentrations of rt-PA, including when rt-PA was absent. Broadband acoustic emissions characteristic of inertial cavitation (Datta et al. 2006) were also present, but at a significantly lower levels (31 ± 5 dB) than UH emissions (Fig. 5b). No correlation between the instantaneous lytic rate and broadband acoustic emissions was established because of the limited range over which broadband acoustic emissions were detected.

The clot was observed to translate synchronously with the initiation and cessations of the ultrasound (Fig. 6 and Video 5). As lysis occurred, the adherence of the clot to the suture was compromised during translation. Hydrodynamic forces of the flow pushed the clot out of the field of view (Video 6). The root-mean-square (RMS) velocity of the clot position was used as a metric to quantify clot motion. The RMS clot velocity was greatest when Definity® and rt-PA were present, however it was not significantly greater than insonation of rt-PA alone ($p > 0.05$). The instantaneous lytic rate correlated significantly ($p < 0.05$) with the RMS velocity of the clot when rt-PA and Definity® were present, as shown in Fig. 7a, but not insonation of Definity® alone ($p > 0.05$). The instantaneous lytic rate also correlated significantly ($p < 0.05$) with the RMS velocity of the clot for insonation of rt-PA alone for all concentrations of rt-PA (Fig. 7b). These data suggest that translation of the clot is generally associated with an increase in the lytic rate when rt-PA is present.

Discussion

An *in vitro* flow model that allows both qualitative observations and real-time, quantitative assessment of the lytic rate was developed for investigating UET mechanisms. Two primary observations were noted in the results of this study. First, clot lysis was found to occur preferentially surrounding large, resonant-sized microbubbles undergoing stable oscillations. UH emissions from these stable oscillations correlated with the instantaneous lytic rate (Fig. 5a). Previous studies have documented microbubble interactions with clots (Acconcia et al.,

2013; Chen et al., 2013), but have not correlated the instantaneous lytic rate with microbubble activity. Furthermore, these studies primarily focused on inertial cavitation, whereas the present study focused on promoting sustained stable cavitation. Other studies have monitored the instantaneous lytic rate while insonating rt-PA (Cheng et al., 2005) or rt-PA and microbubbles (Petit et al., 2012), but did not monitor cavitation emissions. Datta et al. (2006) established a correlation between thrombolytic efficacy and the total dose of UH emissions over a 30 min treatment period *in vitro*, but lacked the ability to track the instantaneous lytic rate. The results of this study suggest that the correlation between UH emissions and thrombolytic efficacy extends to time scales on the order of hundreds of milliseconds. Thus, UH emissions can be used as a real-time metric of sonothrombolytic efficacy.

The second observation of this study is that clots translate synchronously with the initiation and cession of the ultrasound exposure. The RMS velocity of the clot correlates with the lytic rate (Fig. 7). Previous studies have documented the displacement of clots under ultrasound excitation (Wright et al., 2012), but did not assess thrombolytic efficacy. A correlation has previously established between insonation parameters that promote radiation force and thrombolytic efficacy (Francis et al., 1995; Frenkel et al., 2006; Lauer et al., 1992), but lacked a means to quantify clot translation.

During insonation, a wide variety of microbubble activities were observed. Microbubbles were observed to coalesce during acoustic excitation (Fig. 3a–3b), resulting in large, resonant-sized microbubbles (53 μm ± 19 μm). The formation of resonant-sized microbubbles via secondary Bjerknes forces (Leighton, 1995) has been observed previously (Postema et al., 2004). Microbubbles typically persisted on the clot longer than 100 seconds (Fig. 3), which was greater than either the insonation period (50 s) or quiescent period (30 s). There was no discernable change in the size of the persistent microbubbles, suggesting the presence of a stabilizing shell to overcome surface tension (Neppiras, 1980). The persistence of the microbubble resulted in continual lysis during insonation, as evident in Videos 1–3. This suggests sustained microbubble activity, a hallmark of stable cavitation, aids in the enhancement of thrombolytic efficacy for these ultrasound parameters.

The significant correlation between instantaneous UH emissions and thrombolytic efficacy and lytic rate could have a profound influence on the insonation schemes used in future UET studies. The fixed insonification and quiescent periods used in this study require does not optimize the well-known stochastic nature of cavitation (Holt et al., 1994; Lauterborn and Holzfuss, 1991). In addition, the flow rate must be known to determine the quiescent period. Flow rates in highly ischemic middle cerebral arteries can vary between 0–15 cm/s (Alexandrov et al., 2010), but can be as high as 50 cm/s without an occlusion (Reinhard, 2005). Thus, the cavitation optimization routine could be made more robust by real-time feedback to assess the amount of cavitation activity and the presence of cavitation nuclei. Such feedback could ensure the presence of a target instantaneous UH energy and, therefore, maximum lytic rate.

In addition to bubble activity, the clot was seen to translate with the initiation and cessations of the ultrasound (Fig. 6 and Video 5). Wright et al. (2012) and Frenkel et al. (2006)

observed similar translation of whole blood clots, although with focused ultrasound pulses at 1.5 and 1.0 MHz, respectively, and not in the presence of ultrasound contrast agents. Translation of the clot is most likely due to acoustic radiation force (Nyborg, 1953). The acoustic radiation force (F_{RAD}) can be written in terms of the time-averaged intensity of the ultrasound field (I), acoustic absorption (α), and sound speed (c) (Nyborg, 1965):

$$F_{RAD} = \frac{2\alpha I}{c} \quad (3)$$

In the case of fluids, the acoustic radiation force generates acoustic streaming (Lighthill, 1978), whereas in tissues, it causes tissue displacement (Palmeri and Nightingale, 2011). The sound speeds of plasma and human whole blood clots are similar: 1540 m/s (Calor-Filho and Machado, 2006) and 1600 m/s (Nahirnyak et al., 2006), respectively. However, the sound absorption in human whole blood clots is two orders of magnitude larger than plasma (Calor-Filho and Machado, 2006; Nahirnyak et al., 2006). Thus, displacement of the clot by acoustic radiation force should dominate over acoustic streaming. In addition, any adherent or embedded microbubbles (Acconcia et al., 2013) would increase the force (Commander and Prosperetti, 1989; Nyborg, 1965). However, no significant increase was observed in the RMS velocity of the clot during insonation of Definity® and rt-PA in comparison to rt-PA alone. The instantaneous lytic rate was found to correlate significantly with the RMS velocity of the clot ($p < 0.05$). It is unknown whether clot translation would occur *in vivo*, or if this motion is specific to the *in vitro* thrombolysis model used in these studies. Regardless, the correlation between the instantaneous lytic rate and RMS velocity of the clot suggests translation of the clot could be associated with an increase in the lytic rate when rt-PA is present.

No correlation between the instantaneous lytic rate and UH energy or clot translation in the presence of Definity® was observed with these submegahertz -frequency, low-amplitude (less than 0.5 MPa peak to peak) acoustic excitations. The lack of ultrasound-mediated thrombolysis in the absence of rt-PA has previously been observed (Frenkel et al., 2006; Holland et al., 2008; Petit et al., 2012). Other types of ultrasound exposures with higher amplitudes, such as histotripsy (Maxwell et al., 2009) or high intensity focused ultrasound (Borrelli et al., 2012; Chuang et al., 2010; Rosenschein et al., 2000; Westermark et al., 1999), have demonstrated appreciable lysis without a thrombolytic drug. These types of ultrasound exposures rely on the mechanical collapse of inertial cavitation to initiate lysis (Maxwell et al., 2011). The ultrasound scheme employed here, in contrast, relies on the gentle oscillations of stable cavitation to enhance the penetration of the thrombolytic into the clot, and the removal of fibrin degradation products (Datta et al., 2008). No definitive correlation could be established between the instantaneous lytic rate and broadband acoustic emissions from inertial cavitation. Note, however, that the insonation scheme used in this study minimized inertial cavitation and promoted persistent stable cavitation. Such a correlation between the instantaneous lytic rate and inertial cavitation may exist for higher amplitude schemes well above the inertial cavitation threshold, such as histotripsy.

There are several aspects of this *in vitro* study that limits the applicability of these findings *in vivo*. Clearly the composition of the thrombus in the brain during ischemic stroke does not

include a silk suture, and the presence of the suture could potentially alter the clot morphology during formation *in vitro*. The tethered suture does not translate during pulsed insonation in the *in vitro* model. Minimal cavitation activity was detected in the absence of Definity®, and lysis was not observed to occur preferentially around the suture. Thus, the contribution from the suture to clot lysis is probably minimal. This *in vitro* study does not address the potential for embolization of the observed resonant-sized microbubbles, which may occur *in vivo* (Muth and Shank, 2000). The low flow rate considered in this model was fixed, and neglects the contribution of increased flow rates as the clot lyses. The additional shear stresses associated with increased flow rates, as would occur *in vivo*, have previously been shown to increase the lytic rate (Bajd et al., 2010). The acoustic period of 8.33 μs was much shorter than either the frame rate (2.33 Hz, or 0.42 s period) or the shutter speed (16 ms) of the CCD camera. Consequently, any motion acting on this time scale could not be resolved. This limitation could be overcome with high-speed photography studies at frame rates greater than the acoustic period (Bouakaz et al., 2005).

Conclusions

The observations presented here suggest that the process of clot lysis during submegahertz - frequency UET is complex, with a combination of mechanisms contributing to this beneficial bioeffect. The mechanical agitation of clots from ultrasound exposure was sustained over several hundred thousand acoustic cycles. However, the correlation between the lytic rate and UH emissions or translation of the clot indicate these mechanisms act nearly instantaneously to enhance thrombolysis.

Supplementary Material

Refer to Web version on PubMed Central for supplementary material.

Acknowledgments

The authors would like to thank Dr. George J. Shaw and Dr. Jason M. Meunier for their help acquiring human blood for the production of clots. The authors would also like to thank members of the Image-guided Ultrasound Laboratories, especially Dr. Guillaume Bouchoux, for their helpful discussions during the preparation of this manuscript. This work was supported by a grant from the National Institutes of Health (number R01 NS047603).

References

Acconcia C, Leung BYC, Hynynen K, Goertz DE. Interactions between ultrasound stimulated microbubbles and fibrin clots. Appl Phys Lett. 2013; 103:053701.

Alexandrov AV, Molina CA, Grotta JC, Garami Z, Ford SR, Alvarez-Sabin J, Montaner J, Saqqur M, Demchuk AM, Moyé LA. Ultrasound-enhanced systemic thrombolysis for acute ischemic stroke. N Engl J Med. 2004; 351:2170–2178. [PubMed: 15548777]

Alexandrov AV, Tsivgoulis G, Rubiera M, Vadikolias K, Stamboulis E, Molina CA, Alexandrov AW, for the TUCSON Investigators. End-Diastolic Velocity Increase Predicts Recanalization and Neurological Improvement in Patients With Ischemic Stroke With Proximal Arterial Occlusions Receiving Reperfusion Therapies. Stroke. 2010; 41:948–952. [PubMed: 20224054]

Apfel, RE. Acoustic Cavitation. In: Edmonds, PD., editor. Methods in Experimental Physics. Academic Press, Inc; New York: 1981. p. 355-411.

Bajd F, SERŠA I. A Concept of Thrombolysis as a Corrosion-Erosion Process Verified by Optical Microscopy. Microcirculation. 2012; 19:632–641. [PubMed: 22612378]

Bajd F, Vidmar J, Blinc A, Serša I. Microscopic clot fragment evidence of biochemo-mechanical degradation effects in thrombolysis. Thromb Res. 2010; 126:137–143. [PubMed: 20580981]

Blinc A, Francis CW, Trudnowski JL, Carstensen EL. Characterization of ultrasound-potentiated fibrinolysis in vitro. Blood. 1993; 81:2636–2643. [PubMed: 8490172]

Borrelli MJ, O'Brien WD, Hamilton E, Oelze ML, Wu J, Bernock LJ, Tung S, Rokadia H, Culp WC. Influences of Microbubble Diameter and Ultrasonic Parameters on In Vitro Sonothrombolysis Efficacy. J Vasc Interv Radiol. 2012; 23:1677–1684.e1. [PubMed: 23106936]

Bouakaz A, Versluis M, de Jong N. High-speed optical observations of contrast agent destruction. Ultrasound Med Biol. 2005; 31:391–399. [PubMed: 15749563]

Calor-Filho MM, Machado JC. Measurement of the ultrasonic attenuation coefficient of human blood plasma during clotting in the frequency range of 8 to 22 MHz. Ultrasound Med Biol. 2006; 32:1055–1064. [PubMed: 16829319]

Chen X, Leeman JE, Wang J, Pacella JJ, Villanueva FS. New Insights into mechanisms of sonothrombolysis using ultra-high-speed imaging. Ultrasound Med Biol. 2013; 40:258–262. [PubMed: 24139920]

Cheng JY, Shaw GJ, Holland CK. In vitro microscopic imaging of enhanced thrombolysis with 120-kHz ultrasound in a human clot model. Acous Res Lett Onl. 2005; 6:25.

Chuang YH, Cheng PW, Chen SC, Ruan JL, Li PC. Effects of Ultrasound-Induced Inertial Cavitation on Enzymatic Thrombolysis. Ultrasonic Imaging. 2010; 32:81–90. [PubMed: 20687276]

Commander KW, Prosperetti A. Linear pressure waves in bubbly liquids: Comparison between theory and experiments. J Acoust Soc Am. 1989; 85:1–15.

Datta S, Coussios CC, Ammi AY, Mast TD, de Courten-Myers GM, Holland CK. Ultrasound-Enhanced Thrombolysis Using Definity® as a Cavitation Nucleation Agent. Ultrasound Med Biol. 2008; 34:1421–1433. [PubMed: 18378380]

Datta S, Coussios CC, McAdory LE, Tan J, Porter T, De Courten-Myers G, Holland CK. Correlation of cavitation with ultrasound enhancement of thrombolysis. Ultrasound Med Biol. 2006; 32:1257–1267. [PubMed: 16875959]

Devcic-Kuhar B, Pfaffenberger S, Grschl M, Kollmann C, Benes E, Gottsauner-Wolf M. In vitro thrombolysis enhanced by standing and travelling ultrasound wave fields. Ultrasound Med Biol. 2002; 28:1181–1187. [PubMed: 12401389]

Elder SA. Cavitation microstreaming. J Acoust Soc Am. 1959; 31:54–64.

Everbach EC, Francis CW. Cavitational mechanisms in ultrasound-accelerated thrombolysis at 1 MHz. Ultrasound Med Biol. 2000; 26:1153–1160. [PubMed: 11053750]

Flynn, HG. Physics of Acoustic Cavitation in liquids. In: Mason, WP., editor. Physical Acoustics. Academic Press, Inc; New York: 1964. p. 58-172.

Francis CW, Blinc A, Lee S, Cox C. Ultrasound accelerates transport of recombinant tissue plasminogen activator into clots. Ultrasound Med Biol. 1995; 21:419–424. [PubMed: 7645133]

Francis CW, Onundarson PT, Carstensen EL, Blinc A, Meltzer RS, Schwarz K, Marder VJ. Enhancement of fibrinolysis in vitro by ultrasound. J Clin Invest. 1992; 90:2063. [PubMed: 1430229]

Frenkel V, Oberoi J, Stone MJ, Park M, Deng C, Wood BJ, Neeman Z, Horne M III, Li KCP. Pulsed High-Intensity Focused Ultrasound Enhances Thrombolysis in an in Vitro Model 1. Radiology. 2006; 239:86–93. [PubMed: 16493016]

Gibo H, Carver CC, Rhoton AL Jr, Lenkey C, Mitchell RJ. Microsurgical anatomy of the middle cerebral artery. J Neurosurgery. 1981; 54:151–169.

Go AS, Mozaffarian D, Roger VL, Benjamin EJ, Berry JD, Borden WB, Bravata DM, Dai S, Ford ES, Fox CS, Franco S, Fullerton HJ, Gillespie C, Hailpern SM, Heit JA, Howard VJ, Huffman MD, Kissela BM, Kittner SJ, Lackland DT, Lichtman JH, Lisabeth LD, Magid D, Marcus GM, Marelli A, Matchar DB, McGuire DK, Mohler ER, Moy CS, Mussolino ME, Nichol G, Paynter NP, Schreiner PJ, Sorlie PD, Stein J, Turan TN, Virani SS, Wong ND, Woo D, Turner MB, on behalf of the American Heart Association Statistics Committee and Stroke Statistics Subcommittee. Heart Disease and Stroke Statistics–2013 Update: A Report From the American Heart Association. Circulation. 2013; 127:e6–e245. [PubMed: 23239837]

Gonzalez, RC.; Woods, RE. Digital Image Processing. 2. Prentice-Hall; Upper Saddle River: 2002.

Gruber MJ, Bader KB, Holland CK. Cavitation thresholds of contrast agents in an in vitro human clot model exposed to 120-kHz ultrasound. J Acoust Soc Am. 2014; 135:646–653. [PubMed: 25234874]

Hitchcock KE, Ivancevich NM, Haworth KJ, Stamper DNC, Vela DC, Sutton JT, Pyne-Geithman GJ, Holland CK. Ultrasound-enhanced rt-PA Thrombolysis in an ex vivo Porcine Carotid Artery Model. Ultrasound in Medicine & Biolog. 2011; 37:1240–1251.

Holland CK, Vaidya SS, Datta S, Coussios CC, Shaw GJ. Ultrasound-enhanced tissue plasminogen activator thrombolysis in an in vitro porcine clot model. Thromb Res. 2008; 121:663–673. [PubMed: 17854867]

Holt RG, Gaitan DF, Atchley AA, Holzfuss J. Chaotic sonoluminescence. Phys Rev Lett. 1994; 72:1376. [PubMed: 10056697]

Lauer CG, Burge R, Tang DB, Bass BG, Gomez ER, Alving BM. Effect of ultrasound on tissue-type plasminogen activator-induced thrombolysis. Circulation. 1992; 86:1257–1264. [PubMed: 1394932]

Lauterborn W, Holzfuss J. Acoustic Chaos. Int J Bifurcat Chaos. 1991; 1:13–26.

Leighton TG. Bubble population phenomena in acoustic cavitation. Ultrason Sonochemistry. 1995; 2:S123–S136.

Lighthill SJ. Acoustic Streaming. J Sound Vib. 1978; 61:391–418.

Marinkovic SV, Milisavljevic MM, Kovacevic MS, Stevic ZD. Perforating branches of the middle cerebral artery. Microanatomy and clinical significance of their intracerebral segments. Stroke. 1985; 16:1022–1029. [PubMed: 4089920]

Maxwell AD, Cain CA, Duryea AP, Yuan L, Gurm HS, Xu Z. Noninvasive Thrombolysis Using Pulsed Ultrasound Cavitation Therapy – Histotripsy. Ultrasound Med Biol. 2009; 35:1982–1994. [PubMed: 19854563]

Maxwell AD, Owens G, Gurm HS, Ives K, Myers DD Jr, Xu Z. Noninvasive Treatment of Deep Venous Thrombosis Using Pulsed Ultrasound Cavitation Therapy (Histotripsy) in a Porcine Model. J Vasc Interv Radiol. 2011; 22:369–377. [PubMed: 21194969]

Meunier JM, Holland CK, Lindsell CJ, Shaw GJ. Duty cycle dependence of ultrasound enhanced thrombolysis in a human clot model. Ultrasound Med Biol. 2007; 33:576. [PubMed: 17337113]

Molina CA, Barreto AD, Tsivgoulis G, Sierzenski P, Malkoff MD, Rubiera M, Gonzales N, Mikulik R, Pate G, Ostrem J. Transcranial ultrasound in clinical sonothrombolysis (TUCSON) trial. Ann Neurol. 2009; 66:28–38. [PubMed: 19670432]

Muth CM, Shank ES. Gas embolism. N Engl J Med. 2000; 342:476–482. [PubMed: 10675429]

Nahirnyak VM, Yoon SW, Holland CK. Acousto-mechanical and thermal properties of clotted blood. J Acoust Soc Am. 2006; 119:3766. [PubMed: 16838520]

Neppiras EA. Acoustic cavitation. Phys Rep. 1980; 61:159–251.

Ng YS, Stein J, Ning M, Black-Schaffer RM. Comparison of Clinical Characteristics and Functional Outcomes of Ischemic Stroke in Different Vascular Territories. Stroke. 2007; 38:2309–2314. [PubMed: 17615368]

Nyborg WL. Acoustic streaming due to attenuated plane waves. J Acoust Soc Am. 1953; 25:68.

Nyborg, WL. Acoustic Streaming. In: Mason, WP., editor. Physical Acoustics, Physical Acoustics. Academic Press, Inc; Waltham: 1965. p. 265-331.

Palmeri ML, Nightingale KR. Acoustic radiation force-based elasticity imaging methods. Interface Focus. 2011; 1:553–564. [PubMed: 22419986]

Petit B, Gaud E, Colevret D, Arditi M, Yan F, Tranquart F, Allémann E. In vitro sonothrombolysis of human blood clots with BR38 microbubbles. Ultrasound Med Biol. 2012; 38:1222–1233. [PubMed: 22542261]

Postema M, Marmottant P, Lancée CT, Hilgenfeldt S, de Jong N. Ultrasound-induced microbubble coalescence. Ultrasound Med Biol. 2004; 30:1337–1344. [PubMed: 15582233]

Prokop AF, Soltani A, Roy RA. Cavitational Mechanisms in Ultrasound-Accelerated Fibrinolysis. Ultrasound Med Biol. 2007; 33:924–933. [PubMed: 17434661]

Reinhard M. Dynamic Cerebral Autoregulation in Acute Ischemic Stroke Assessed From Spontaneous Blood Pressure Fluctuations. Stroke. 2005; 36:1684–1689. [PubMed: 16020768]

Rosenschein U, Furman V, Kerner E, Fabian I, Bernheim J, Eshel Y. Ultrasound Imaging-Guided Noninvasive Ultrasound Thrombolysis : Preclinical Results. Circulation. 2000; 102:238–245. [PubMed: 10889137]

Saqqur M, Uchino K, Demchuk AM, Molina CA, Garami Z, Calleja S, Akhtar N, Orouk FO, Salam A, Shuaib A, Alexandrov AV, for CLOTBUST Investigators. Site of Arterial Occlusion Identified by Transcranial Doppler Predicts the Response to Intravenous Thrombolysis for Stroke. Stroke. 2007; 38:948–954. [PubMed: 17290031]

Shaw GJ, Bavani N, Dhamija A, Lindsell CJ. Effect of mild hypothermia on the thrombolytic efficacy of 120 kHz ultrasound enhanced thrombolysis in an in-vitro human clot model. Thromb Res. 2006; 117:603–608. [PubMed: 15951005]

Shaw GJ, Dhamija A, Bavani N, Wagner KR, Holland CK. Arrhenius temperature dependence of in vitrotissue plasminogen activator thrombolysis. Phys Med Biol. 2007; 52:2953–2967. [PubMed: 17505082]

Shaw GJ, Meunier JM, Huang SL, Lindsell CJ, McPherson DD, Holland CK. Ultrasound-enhanced thrombolysis with tPA-loaded echogenic liposomes. Thromb Res. 2009a; 124:306–310. [PubMed: 19217651]

Shaw GJ, Meunier JM, Lindsell CJ, Holland CK. Tissue Plasminogen Activator Concentration Dependence of 120 kHz Ultrasound-Enhanced Thrombolysis. Ultrasound Med Biol. 2008; 34:1783–1792. [PubMed: 18468773]

Shaw GJ, Sperling M, Meunier JM. Long-term stability of recombinant tissue plasminogen activator at −80 C. BMC Res Notes. 2009b; 2:117. [PubMed: 19566947]

Sutton JT, Haworth KJ, Pyne-Geithman G, Holland CK. Ultrasound-mediated drug delivery for cardiovascular disease. Expert Opin Drug Deliv. 2013; 10:573–592. [PubMed: 23448121]

Turi ZG, Goldberg S, LittleJohn JK, VanderArk C, Shadoff N, Karlsberg R, Williams J, Butman S, Stadius ML, Wise K. Dose-related efficacy and bleeding complications of double-chain tissue plasminogen activator in acute myocardial infarction. Am J Cardiol. 1993; 71:1009–1014. [PubMed: 8475860]

Westermark S, Wiksell H, Elmqvist H, Hultenby K, Berglund H. Effect of externally applied focused acoustic energy on clot disruption in vitro. Clin Sci. 1999; 97:67–71. [PubMed: 10369795]

Wright CC, Hynynen K, Goertz DE. Pulsed Focused Ultrasound-Induced Displacements in Confined In Vitro Blood Clots. IEEE Trans Biomed Eng. 2012; 59:842–851. [PubMed: 22194235]

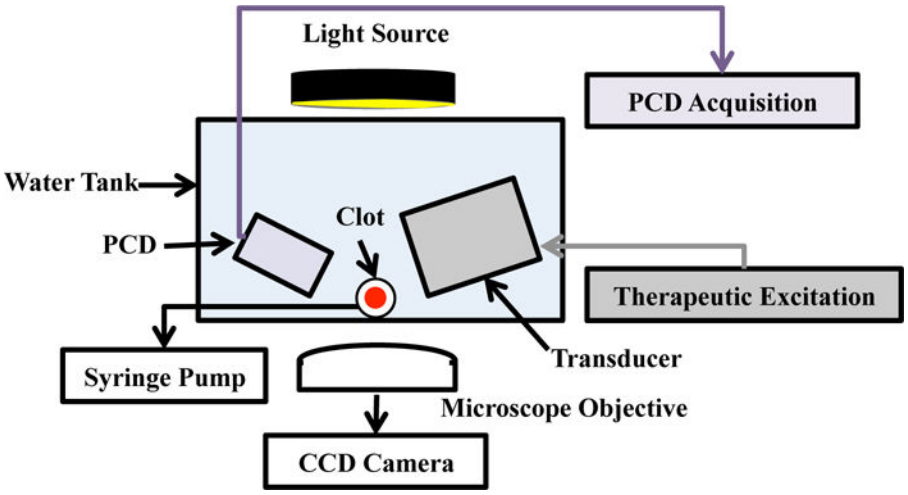

Figure 1.
Experimental set-up for observation of ultrasound-enhanced thrombolysis.

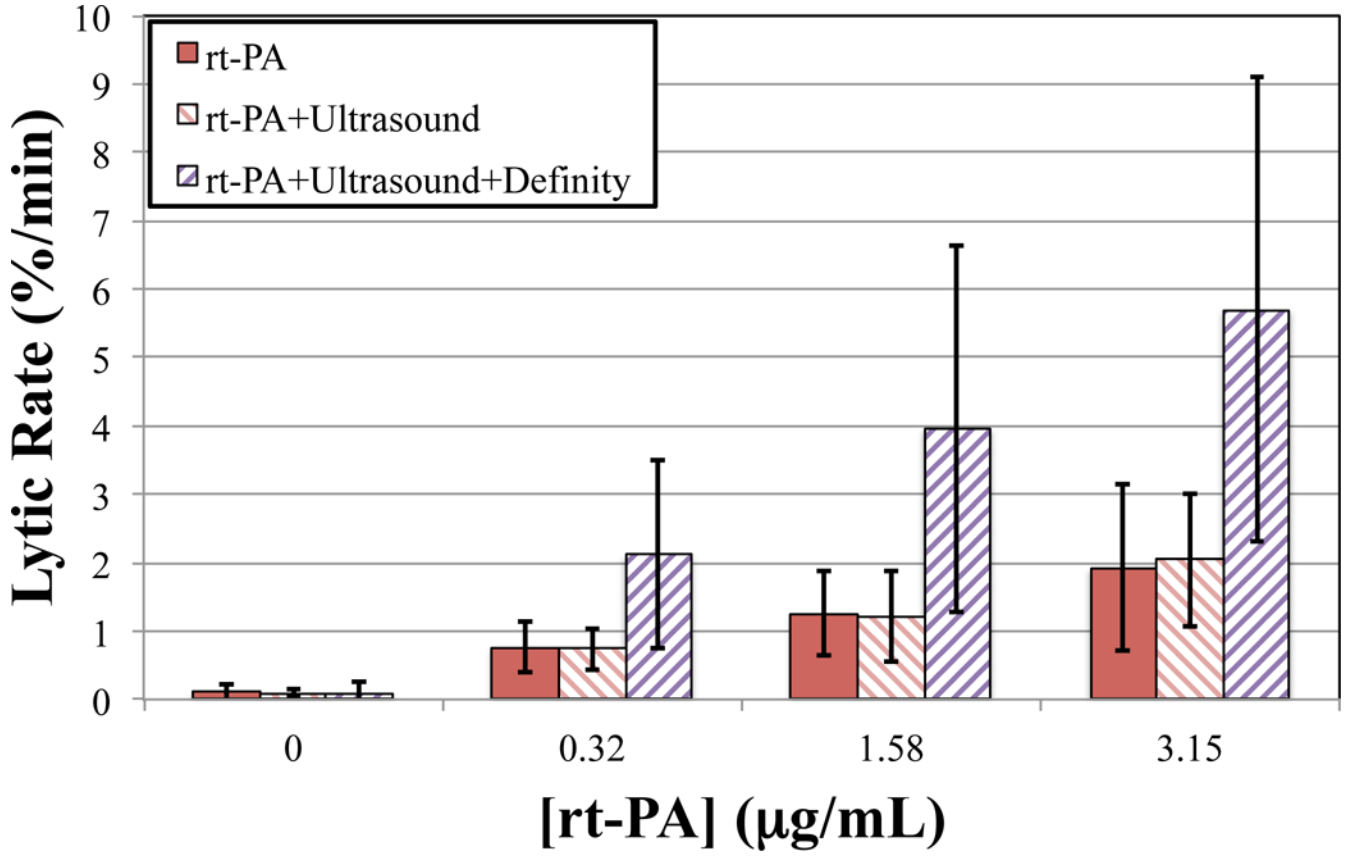

Figure 2.

The average lytic rate over the 30 min treatment duration at each concentration of recombinant tissue-type plasminogen activator (rt-PA), computed using Equation (1) at t_1 = 0min and t_2 = 30 min. Clots were exposed to rt-PA, rt-PA and ultrasound, and rt-PA, US, and Definity®.

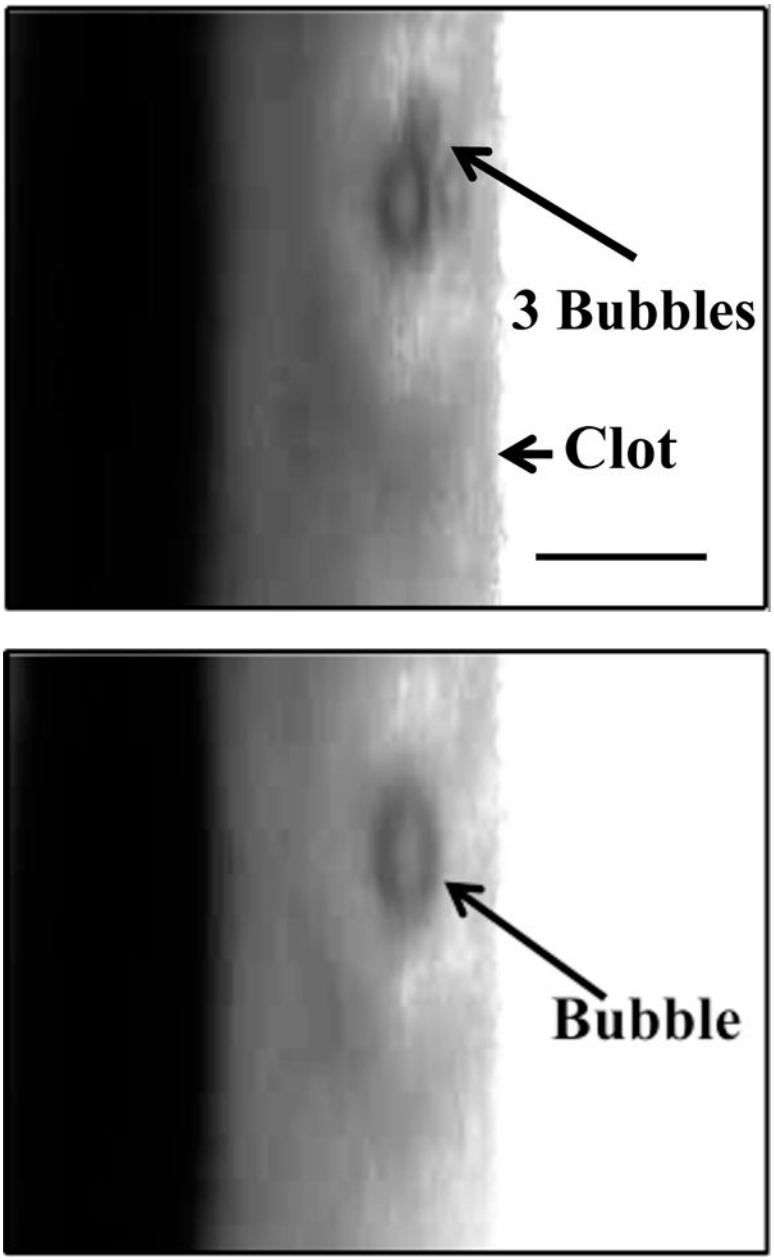

Figure 3.

Coalescence and translation of bubble. (***a***) Prior to insonation, three bubbles are visible on the clot. (***b***) The three bubble coalesce within 400 ms after ultrasound exposure. (***c***) The resultant bubble translates after remaining stationary for 3.5 s. The surrounding fluid contains recombinant tissue-type plasminogen activator (0.32 μg/mL), and Definity® (2 μL/mL). The bubble appears distorted due to the long exposure time of the camera (16 ms) compared to the acoustic period (8.33 μs). The scale bar in panel ***a*** is 100 μm.

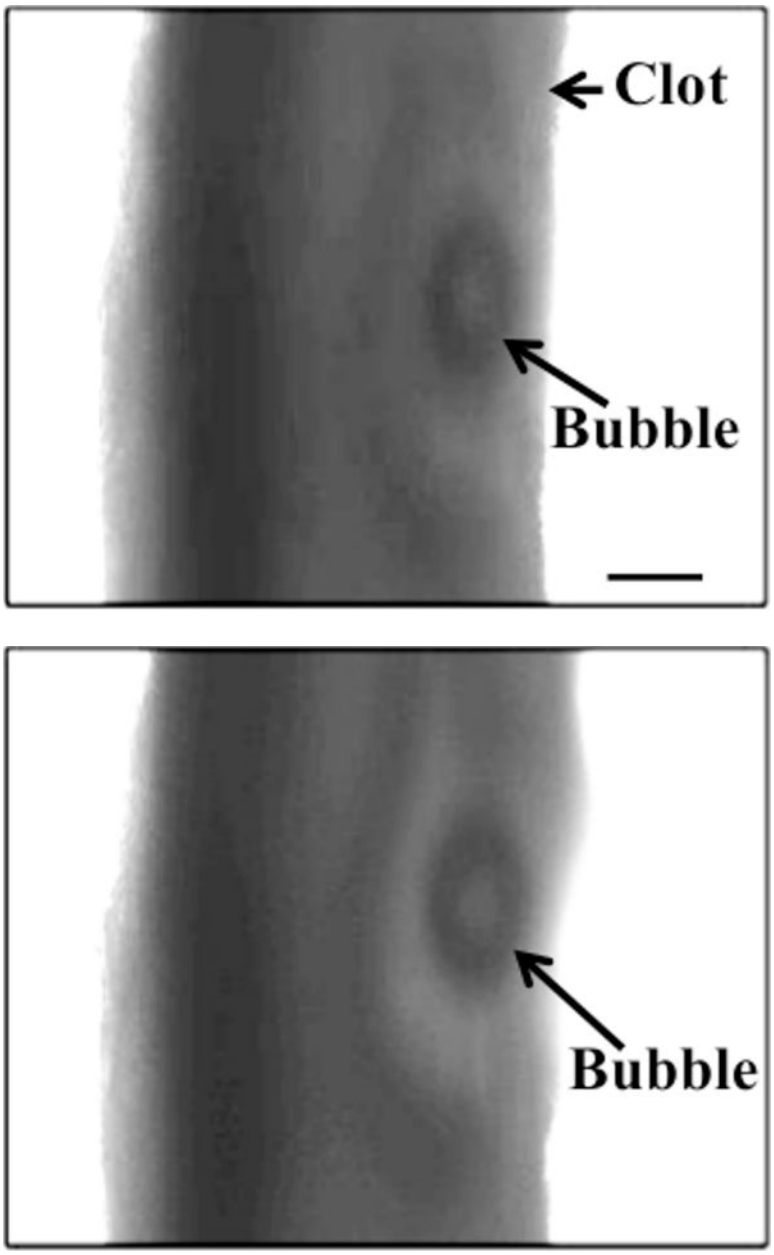

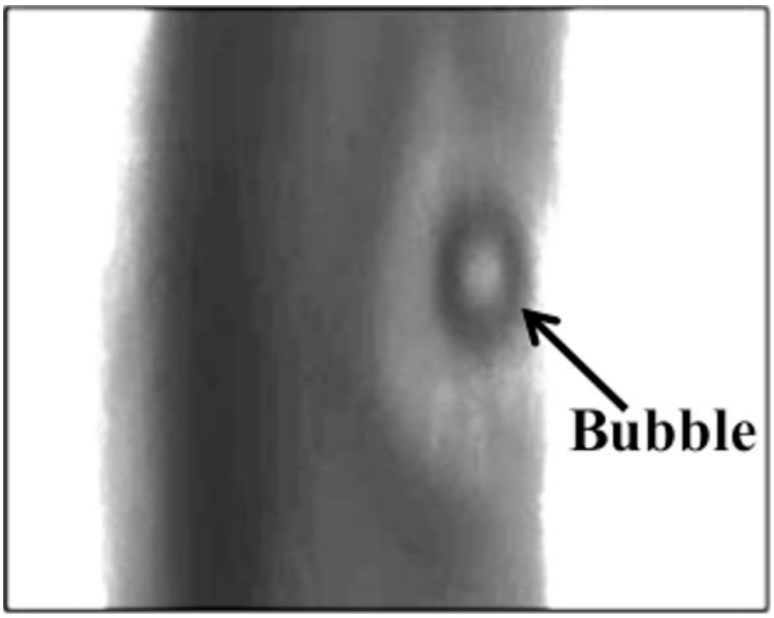

Figure 4.

Increase in pixel intensity surrounding stable oscillations of acoustically activated bubble. Lysis occurs over a long time scale compared to the acoustic period (interframe time is 1.7 s, acoustic period is 8.33 μs). The effluent surrounding the clot is human fresh-frozen plasma, recombinant tissue-type plasminogen activator (1.58 μg/mL), and Definity® (2 μL/mL). The ultrasound (120 kHz, 0.44 MPa continuous wave) is on during panels **a–c**. The bubble appears distorted due to the long exposure time of the camera (16 ms) compared to the acoustic period (8.33 μs).

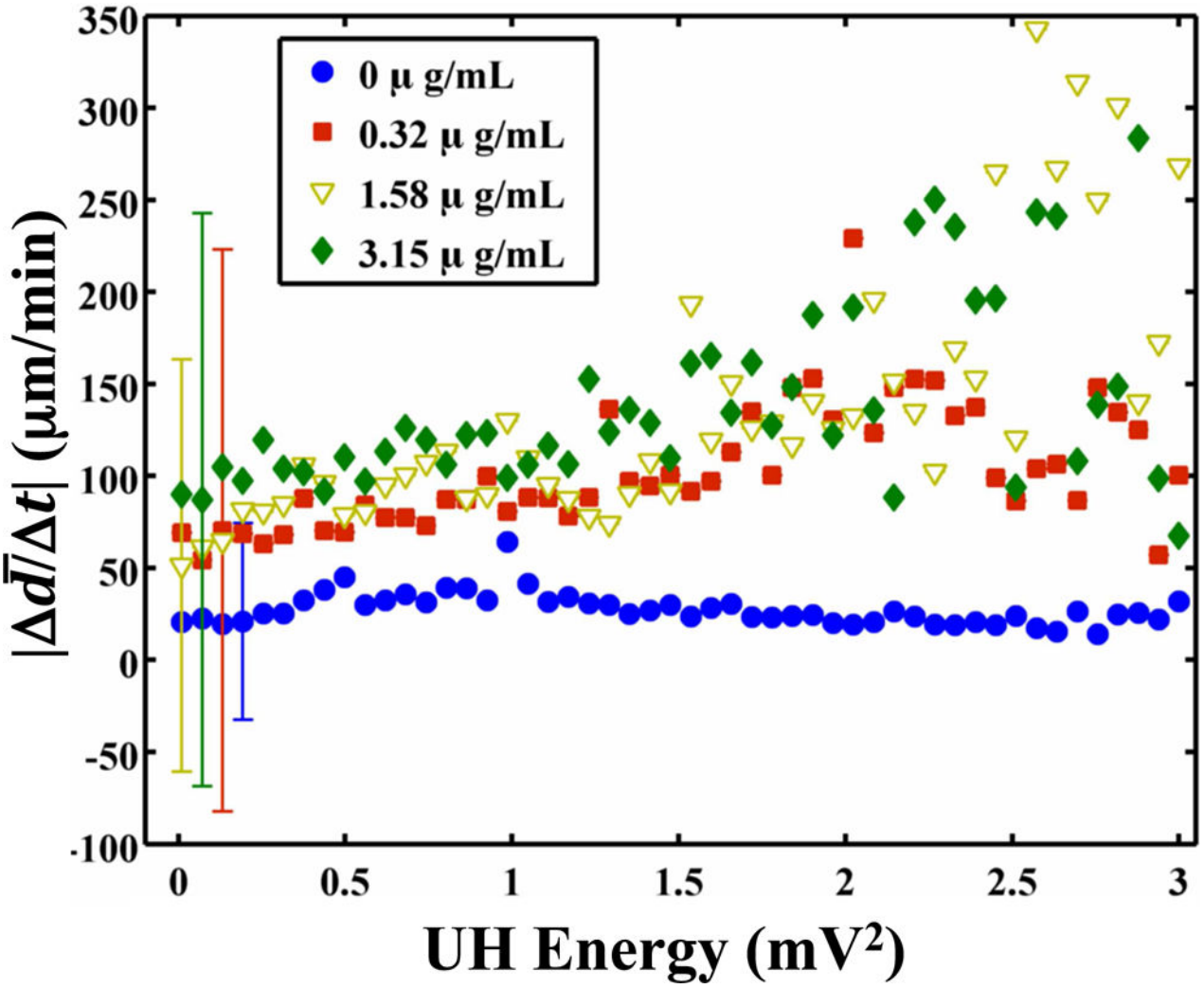

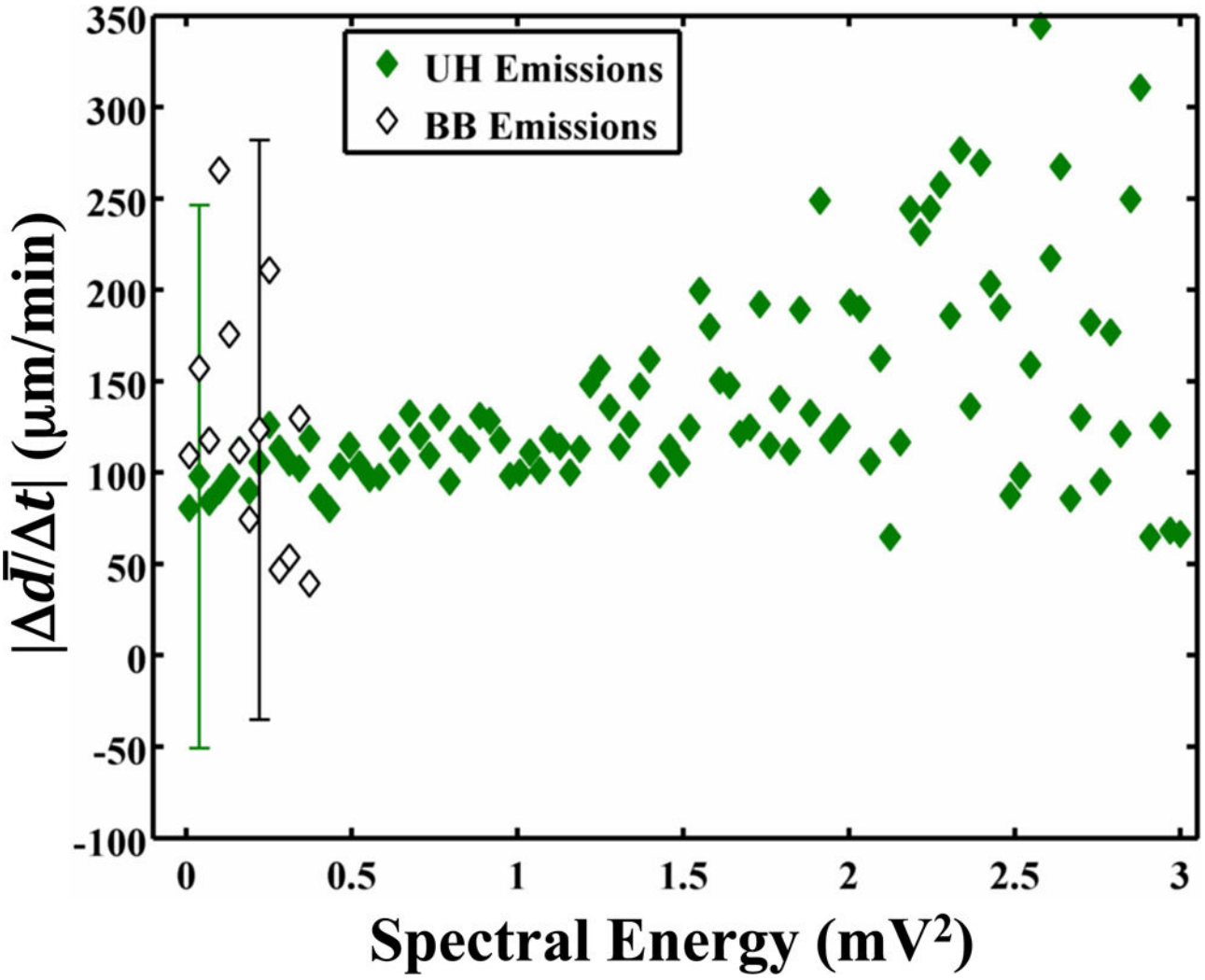

Figure 5.

(*a*) The absolute lytic rate ($|\Delta\bar{d}/\Delta t|$) as a function of the UH energy at each concentration of recombinant tissue-type plasminogen activator (rt-PA). The lytic rate was computed using Equation (1), with $t_2 - t_1 = 0.43$ s, the interframe time of the clot images. The error bars are representative of the standard deviation of the lytic rate over a 0.05 mV^2 range of UH energies. The lytic rate significantly correlates ($p < 0.05$) with the UH energy when rt-PA is present. (*b*) The absolute lytic rate ($|\Delta\bar{d}/\Delta t|$) as a function of ultraharmonic (UH) and broadband (BB) energy at an rt-PA concentration of 3.15 μg/mL. The lytic rate was computed using Equation (1), with $t_2 - t_1 = 0.43$ s, the interframe time of the clot images. The error bars are representative of the standard deviation of the lytic rate over a 0.03 mV^2 range of UH energies.

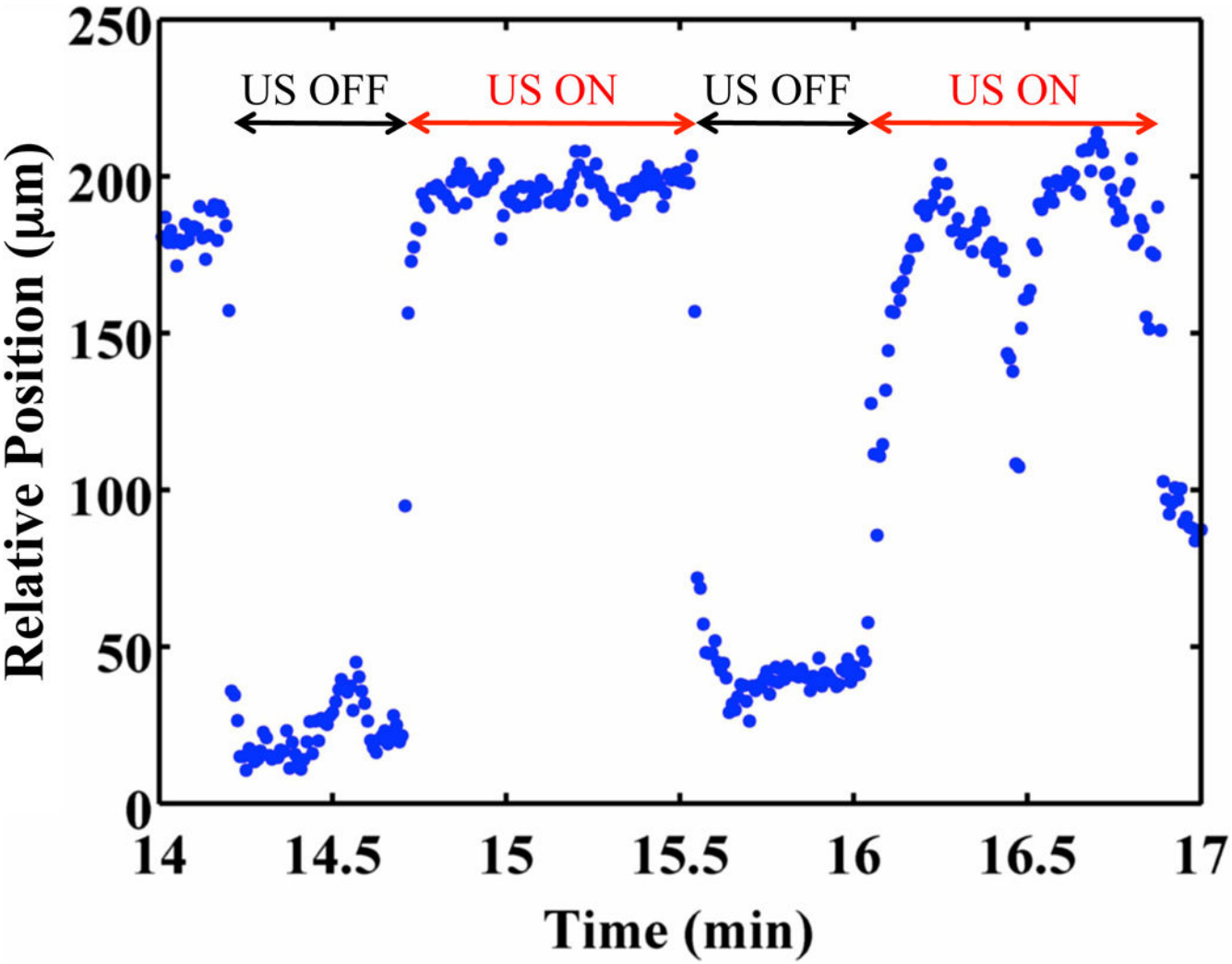

Figure 6.

Clot position as function of time. The clot position was 0 μm at time 0 min. The clot was exposed to 0.32 μg/mL recombinant tissue-type plasminogen activator, submegahertz - frequency ultrasound, and 2 μL/mL Definity®. Positive position values indicate movement along the direction of propagation of the ultrasound (i.e. away from the transducer).

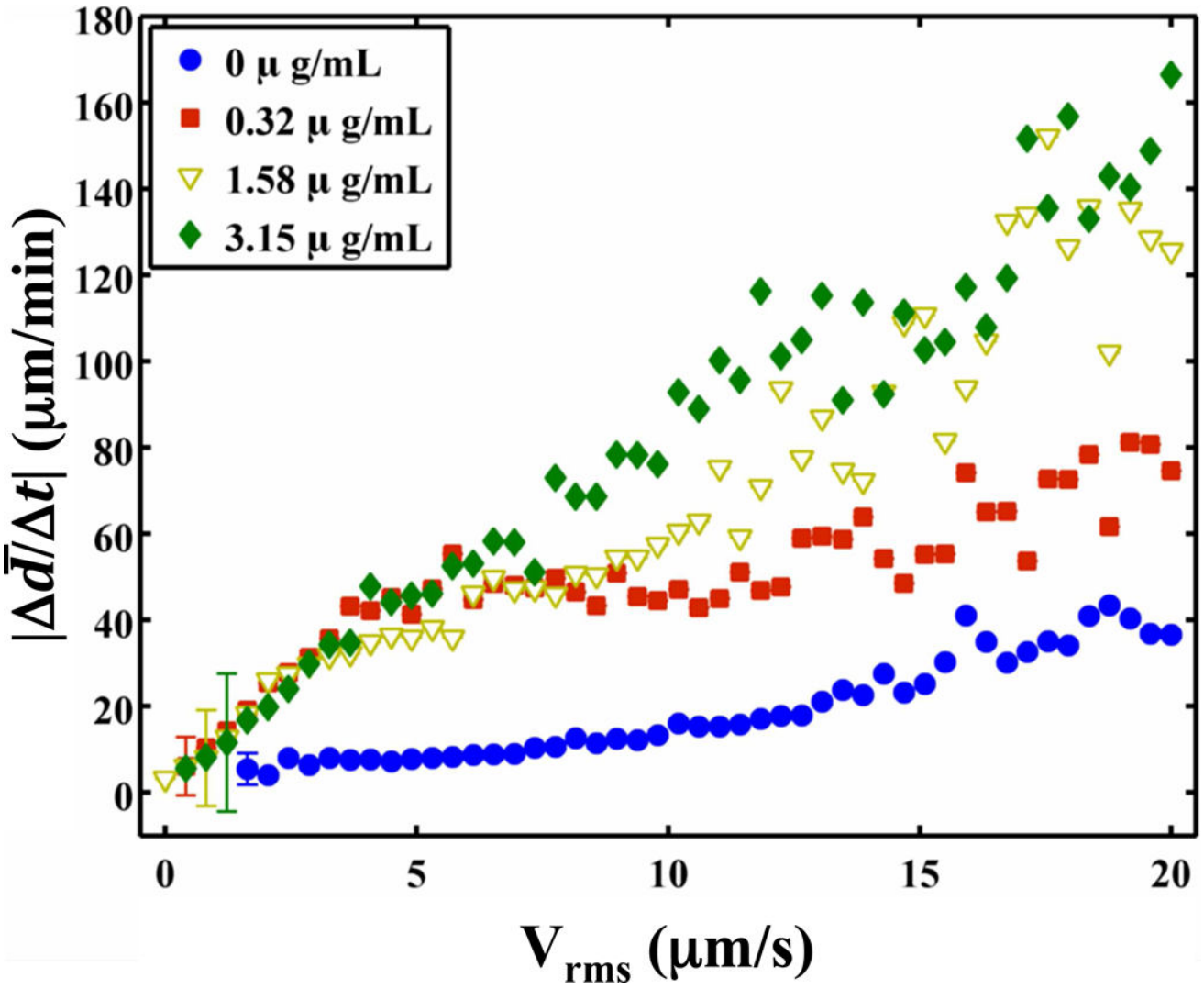

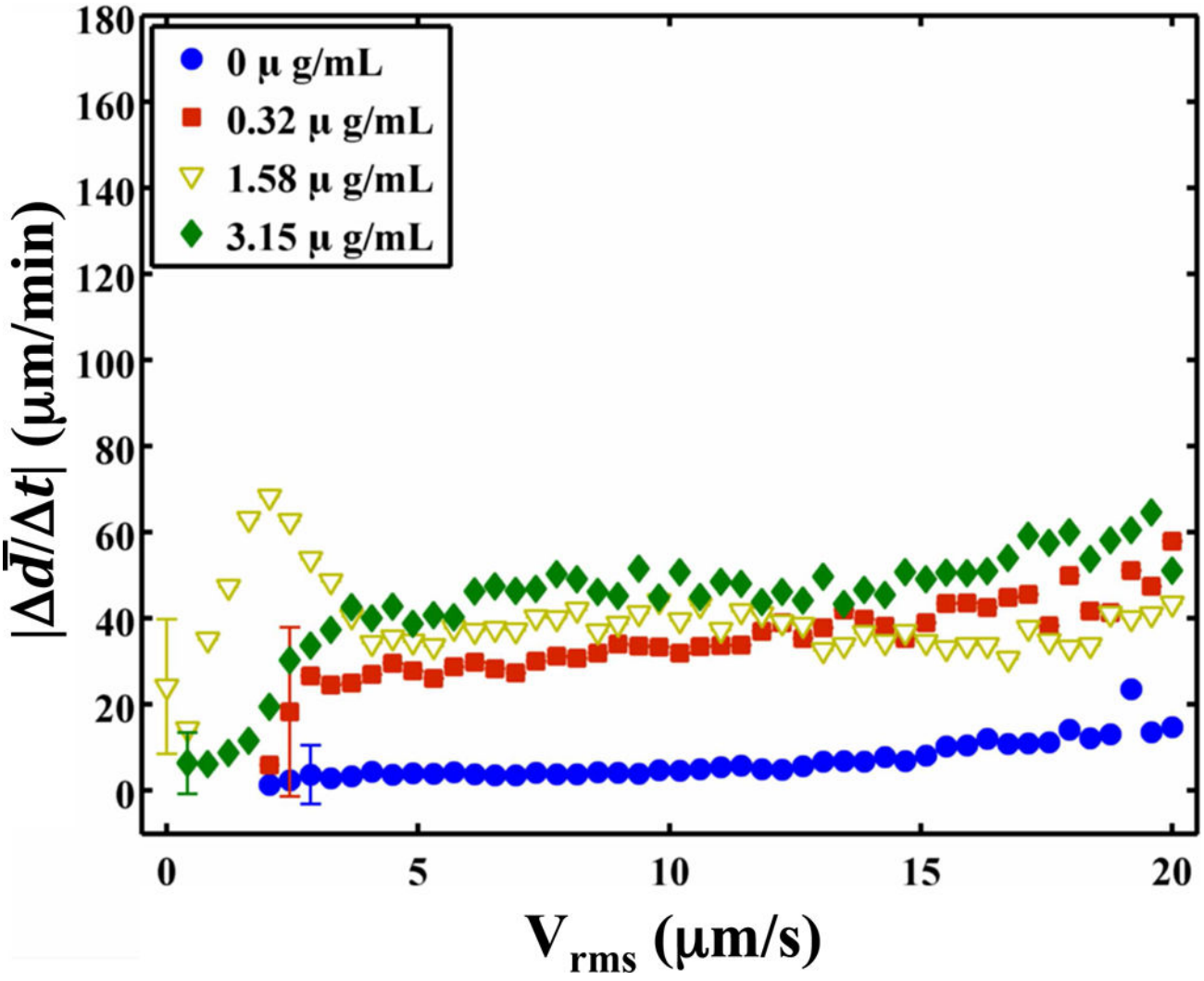

Figure 7.

The absolute lytic rate ($|\Delta\bar{d}/\Delta t|$) as a function of the RMS velocity of the clot at each concentration of recombinant tissue-type plasminogen activator (rt-PA). The lytic rate was computed using Equation (1), with $t_2 - t_1 = 0.43$ s, the interframe time of the clot images. Similarly, the RMS velocity of the clot was computed using Equation (2), with $t_2 - t_1 = 0.43$ s. The error bars are representative of the standard deviation of the lytic rate over a 0.41 μm/s range of RMS velocities. ***(a)*** Insonation of rt-PA and Definity®. The lytic rate significantly correlates ($p < 0.05$) with the RMS velocity when rt-PA is present. ***(b)*** Insonation of rt-PA alone. The lytic rate significantly correlates ($p < 0.05$) with the RMS velocity at all concentrations of rt-PA.